Since January 2020 Elsevier has created a COVID-19 resource centre with free information in English and Mandarin on the novel coronavirus COVID-19. The COVID-19 resource centre is hosted on Elsevier Connect, the company's public news and information website.

Pharmacological Research 161 (2020) 105223

Contents lists available at ScienceDirect

Pharmacological Research

journal homepage: www.elsevier.com/locate/yphrs

Activation of angiotensin II type-2 receptor protects against cigarette smoke-induced COPD

Dan Mei [a], W.S. Daniel Tan [a], Wupeng Liao [a], C.K. Matthew Heng [a], W.S. Fred Wong [a,b,c,*]

[a] Department of Pharmacology, Yong Loo Lin School of Medicine, National University Health System, 117600, Singapore
[b] Immunology Program, Life Science Institute, National University of Singapore, 117456, Singapore
[c] Singapore-HUJ Alliance for Research and Enterprise, National University of Singapore, 138602, Singapore

ARTICLE INFO

Keywords:
Angiotensin-(1-7)
Angiotensin-Converting enzyme
Antioxidant
Emphysema
Mas receptor
Phosphatases

Chemical compounds studied in this article:
Compound 21 (CID: 9804984)

ABSTRACT

Chronic obstructive pulmonary disease (COPD) is the third leading cause of death globally. Cumulative evidence has implicated renin-angiotensin system (RAS) in the pathogenesis of COPD. This study aimed to investigate potential protective effects of angiotensin II type-2 receptor (AT2R) activation in cigarette smoke (CS)-induced COPD models. Compound 21 (C21), a selective and potent non-peptide small molecule AT2R agonist, was evaluated for anti-inflammatory, anti-oxidative and anti-remodeling activities in a two-week (acute) and an eight-week (chronic) CS-induced COPD models. C21 inhibited CS-induced increases in macrophage and neutrophil counts, pro-inflammatory cytokines and oxidative damage markers in bronchoalveolar lavage (BAL) fluid, and TGF-β1 in lung tissues, from COPD models. C21 restored phosphatase activities and reduced phospho-p38 MAPK, phospho-ERK and p65 subunit of NF-κB levels in CS-exposed lung tissues. C21 also suppressed CS-induced increases in *α-Sma*, *Mmp9*, *Mmp12* and hydroxyproline levels in lung tissues, and neutrophil elastase activity in BAL fluid. C21 modulated RAS in CS-exposed lungs by downregulating Ang II but upregulating Ang-(1–7) and Mas receptor levels. C21 prevented CS-induced emphysema and improved lung functions in chronic COPD model. We report here for the first time the protective effects of AT2R agonist C21 against CS-induced COPD, and provide strong evidence for further development of AT2R agonist for the treatment of COPD.

1. Introduction

Chronic obstructive pulmonary disease (COPD) is characterized by alveolar space enlargement and airway remodeling, leading to breathlessness and impaired lung function [1]. COPD ranks third in the global leading cause of death, with 3.2 million deaths in 2017. Annual mortality from COPD is estimated to reach 4.4 million by 2040 [2]. Cigarette smoking is the major risk factor for COPD, which delivers huge amount of reactive oxygen and nitrogen species into the lungs that incite production of inflammatory cytokines like IL-1β, IL-6 and TNF-α, and infiltration of inflammatory cells like macrophages and neutrophils [3,4]. Infiltrated neutrophils and macrophages are the major sources of endogenous free radicals generated by enzymes like myeloperoxidase and NADPH oxidase [4,5], which accentuate excessive oxidative damage to the lungs [6,7]. Current COPD therapeutics fail to stop the progression of the disease or reduce the mortality. Most COPD patients are also corticosteroid-insensitive [8]. There is an urgent need to discover novel therapeutic strategies for the treatment of COPD.

Renin-angiotensin system (RAS) plays a central role in regulating blood pressure and electrolyte homeostasis [9,10]. More recently, cumulative evidence has implicated RAS in the pathogenesis of COPD [11,12]. Renin, an endopeptidase, cleaves angiotensinogen into angiotensin I (Ang I) decapeptide which, in turns, is cleaved by angiotensin converting enzyme (ACE), a zinc metallopeptidase, into Ang II octapeptide. Ang II is subsequently cleaved by ACE2, a homologue of ACE, into Ang-(1–7) [9,10]. Ang II can bind and activate G protein-coupled receptors (GPCRs) Ang II type-1 receptor (AT1R) and Ang II type-2 receptor (AT2R), while Ang-(1–7) binds and activates G protein-coupled Mas receptor. AT1R activation not only leads to vasoconstriction and renal retention of electrolytes and water, but also promotes inflammation, proliferation and fibrosis [11]. In contrast, activation of AT2R and Mas receptor mediates opposing effects including vasodilatory, anti-proliferative, anti-oxidative, anti-inflammatory and anti-fibrotic actions [11,12]. AT1R blockers have been shown to antagonize TGF-β

* Corresponding author at: Department of Pharmacology, Yong Loo Lin School of Medicine, 04-01H, MD3, 16 Medical Drive, National University Health System, 117600, Singapore.
E-mail address: phcwongf@nus.edu.sg (W.S.F. Wong).

https://doi.org/10.1016/j.phrs.2020.105223
Received 27 July 2020; Received in revised form 13 September 2020; Accepted 23 September 2020
Available online 2 October 2020

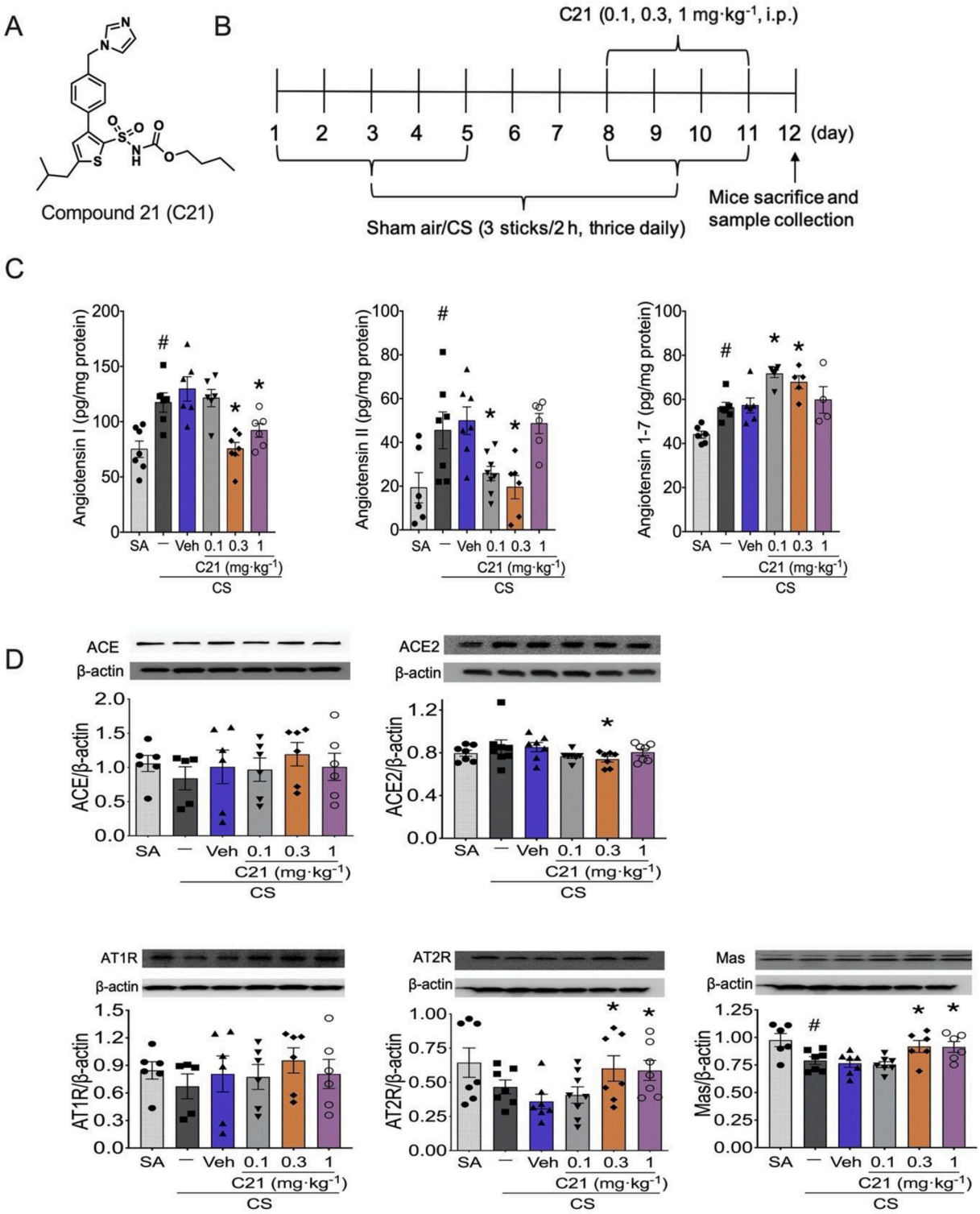

Fig. 1. Modulatory effects of AT2R agonist C21 on RAS in a CS-induced acute lung injury mouse model. (A) Chemical structure of compound 21. (B) Experimental protocol for the 2-week CS-induced acute lung injury model. C21 was given once daily 1 h before CS exposure. (C) Effects of C21 on the levels of Ang I, Ang II and Ang-(1-7) in lung tissues from CS-challenged mice (n = 4-8). (D) Effects of C21 on the expression of ACE, ACE2, AT1R, AT2R and Mas receptor in lung tissues from CS-challenged mice (n = 5-8). Values are expressed as mean ± SEM. #: $p < 0.05$ compared with sham air control, *: $p < 0.05$ compared with vehicle DMSO control.

signaling, attenuate alveolar cell apoptosis, emphysema, metalloprotease activation and epithelial hyperplasia, and increase running distance in mouse models of COPD [13,14]. Population-based clinical studies have revealed that the use of AT1R blockers was associated with slower progression of percent emphysema in general population, especially in former smokers [15], and with lower risk of pneumonia and lower mortality in COPD patients [16,17]. On the other hand, Ang-(1–7), by activating Mas receptors, exhibited anti-inflammatory, anti-oxidative and anti-fibrotic actions, restored autophagic functions, and improved locomotor activity in mouse models of COPD [18–20]. The role of AT2R in COPD is unknown. The purpose of the present study was to investigate potential protective effects of AT2R activation in

cigarette smoke (CS)-induced COPD mouse models.

Compound 21 (C21) is the first non-peptide AT2R-selective small molecule agonist with an AT2R affinity constant of 4×10^{-10} M and AT1R affinity constant of 1×10^{-5} M, exhibiting >25,000-fold selectivity for AT2R [21,22]. C21 contains a biaryl privileged structure with isobutyl lipophilic side chain, a sulfonylcarbamate group and a methylene imidazole moiety to induced AT2R conformational change during receptor activation (Fig. 1A) [23]. C21 has been shown to lower infiltrated macrophages, lung inflammation, collagen deposition, muscularization of pulmonary vessels and right ventricular remodeling in a bleomycin-induced lung injury rat model [24]. C21 has been tested in a Phase I clinical trial and is confirmed to be safe and well-tolerated in humans [25]. The present study reported for the first time the benefits of AT2R activation that C21 exhibited anti-inflammatory, anti-oxidative, anti-remodeling and lung function restoration actions in acute and chronic CS-induced COPD models.

2. Materials and methods

2.1. Acute and chronic cigarette-smoking mouse models

Female BALB/c mice of 6–8 weeks old (InVivos Pte. Ltd., Singapore) were placed in a ventilated chamber and exposed to 5% CS from 3 sticks of 3R4F research cigarettes (Tobacco and Health Research Institute, University of Kentucky, Lexington, KY) for 20 min three times daily at 2 h interval 5 days per week for 2 weeks to develop the CS-induced acute lung injury model as described [26] (Fig. 1B). Sham air controls were mice placed in a separate ventilated chamber exposed to room air only. C21 (Axon Medchem BV, Groningen, The Netherlands; 0.1, 0.3 and 1 mg· kg^{-1}) (Fig. 1A) or vehicle control (0.33 % DMSO; Sigma-Aldrich, St. Louis, USA) were prepared in 0.1 mL saline and given i.p. once daily 1 h before CS exposure in the second week. For the chronic CS model, same smoking protocol in mice was extended to 8 weeks, and C21 (0.3 mg· kg^{-1}) was given once daily 1 h before CS exposure in the last three weeks as described [26] (Fig. 5A). Mice were sacrificed 24 h after the last CS exposure for analyses. Animal experiments were performed according to the guidelines of the Institutional Animal Care and Use Committee of the National University of Singapore.

2.2. Bronchoalveolar lavage (BAL) fluid analysis

Mice were anaesthetized using 400 μL of anesthetic mixture (7.5 mg· mL^{-1} ketamine + 0.1 mg· mL^{-1} medetomidine) by i.p. injection. Tracheotomy was performed and a cannula was inserted into the trachea. Ice cold PBS (0.5 mL × 3) was instilled into the lungs and the BAL fluid was collected for cell counts, neutrophil elastase (NE) activity and ELISA analysis.

2.3. Lung tissue analyses

Lung tissues were homogenized in PBS using a ceramic bead-based homogenizer (Bertin Corporation, Precellys, MD, USA). Supernatants were assayed for Ang I (Reddot Biotech, Kelowna, Canada), Ang II (Sigma-Aldrich), Ang-(1–7) (Cusabio, Wuhan, Hubei, China), TGF-β1 (Thermo Fisher Scientific, Waltham, MA, USA), phosphatase activity (Thermo Fisher Scientific) and SHP-2 phosphatase activity (BPS Bioscience, San Diego, CA, USA). Total lung protein lysates were also prepared using T-PER buffer (Thermo Fisher Scientific), separated by 10 % SDS–PAGE and immunoblotted with anti-AT1R, anti-AT2R, anti-Mas, anti-ACE or anti-ACE2 antibodies (Abcam, Cambridge, MA, USA), anti-phospho-p38, anti-p38, anti-phospho-ERK, anti-ERK or anti-p65 antibodies (Cell Signaling Technology, Danvers, MA, USA), or anti-β-actin (Proteintech, Rosemont, IL, USA). ImageJ software (National Institute of Health, Bethesda, MD, USA) was used to quantitate protein band intensity. Total RNA was extracted with RNAzol reagent (Molecular Research Center Inc., Cincinnati, OH, USA) and then used for first strand cDNA synthesis. The PCR primer sequences (Integrated DNA Technologies, Coraville, IA, USA) are shown in the Table 1. Template cDNA (100 ng) in the PCR mixture containing Fast SYBR Green Master Mix (Applied Biosystems, Carlsbad, CA, USA) was amplified and quantitated using a sequence detector (ABI 7500 cycler, Applied Biosystems). The mRNA expression levels for all targets were normalized to a housekeeping gene HPRT.

Table 1
Mouse primer sequences used in this study.

Gene	Primer	Sequence (5′-3′)
Mmp9	Forward	CGCTCATGTACCCGCTGTAT
	Reverse	TGTCTGCCGGACTCAAAGAC
Mmp12	Forward	CATGAAGCGTGAGGATGTAGAC
	Reverse	TGGGCTAGTGTACCACCTTTG
Nqo-1	Forward	AGAGAGTGCTCGTAGCAGGAT
	Reverse	GTGGTGATAGAAAGCAAGGTCTT
Gsr	Forward	GCGTGAATGTTGGATGTGTACC
	Reverse	GTTGCATAGCCGTGGATAATTTC
Ho-1	Forward	AAGCCGAGAATGCTGAGTTCA
	Reverse	GCCGTGTAGATATGGTACAAGGA
Gpx2	Forward	ATGGCTTACATTGCCAAGTCG
	Reverse	TGCCTCTGAACGTATTGAAGTC
α-Sma	Forward	TCAGCAAACAGGAATACGACGA
	Reverse	TTGGAAAGGAACTGGAGGCG
Timp1	Forward	GGGCATATCCACAGAGGCTTT
	Reverse	GTGGGAAATGCCGCAGAT
Muc5ac	Forward	CTGTGACATTATCCCATAAGCCC
Muc5b	Reverse	AAGGGGTATAGCTGGCCTGA
	Forward	TCCCTAGCATGAGCGCCTTA
	Reverse	CCACGACGCAGTTGGATGTT

2.4. Histology

Lungs were fixed in 10 % neutral formalin, paraffinized, cut into 5-μm sections, and stained with hematoxylin and eosin (H & E) for examining airway inflammation and scoring epithelium thickness and alveolar enlargement, performed in a blinded manner as described previously [26,27].

2.5. Lung function analysis

For the chronic CS exposure model, mice were anaesthetized with 150 μL of the same anesthetic mixture by i.p. injection, followed by tracheotomy as described [26]. Mice were placed in a whole-body plethysmograph connected to a computer-controlled ventilator (Forced Pulmonary Maneuver System, Buxco Research System, Wilmington, NC, USA) [26]. Lung functions were recorded using the FinePointe™ data acquisition and analysis software (Buxco Research System).

2.6. Statistical analyses

Data are presented as mean ± SEM. Significant difference between treatment groups was determined by one-way ANOVA followed by Dunnett's test. Significant level was set at $p < 0.05$. All statistical analyses were conducted with GraphPad Prism software. $^{\#}$indicates $p < 0.05$ when CS group compared to sham air control group; whereas, *indicates $p < 0.05$ when C21-treated groups compared to vehicle control.

3. Results

3.1. AT2R activation modulates RAS in acute CS exposure

Ang I, Ang II and Ang-(1–7) levels were significantly upregulated in the lungs in response to CS challenge. Among the doses used, C21 at 0.3 mg· kg^{-1} could markedly revert Ang I and Ang II back to basal levels,

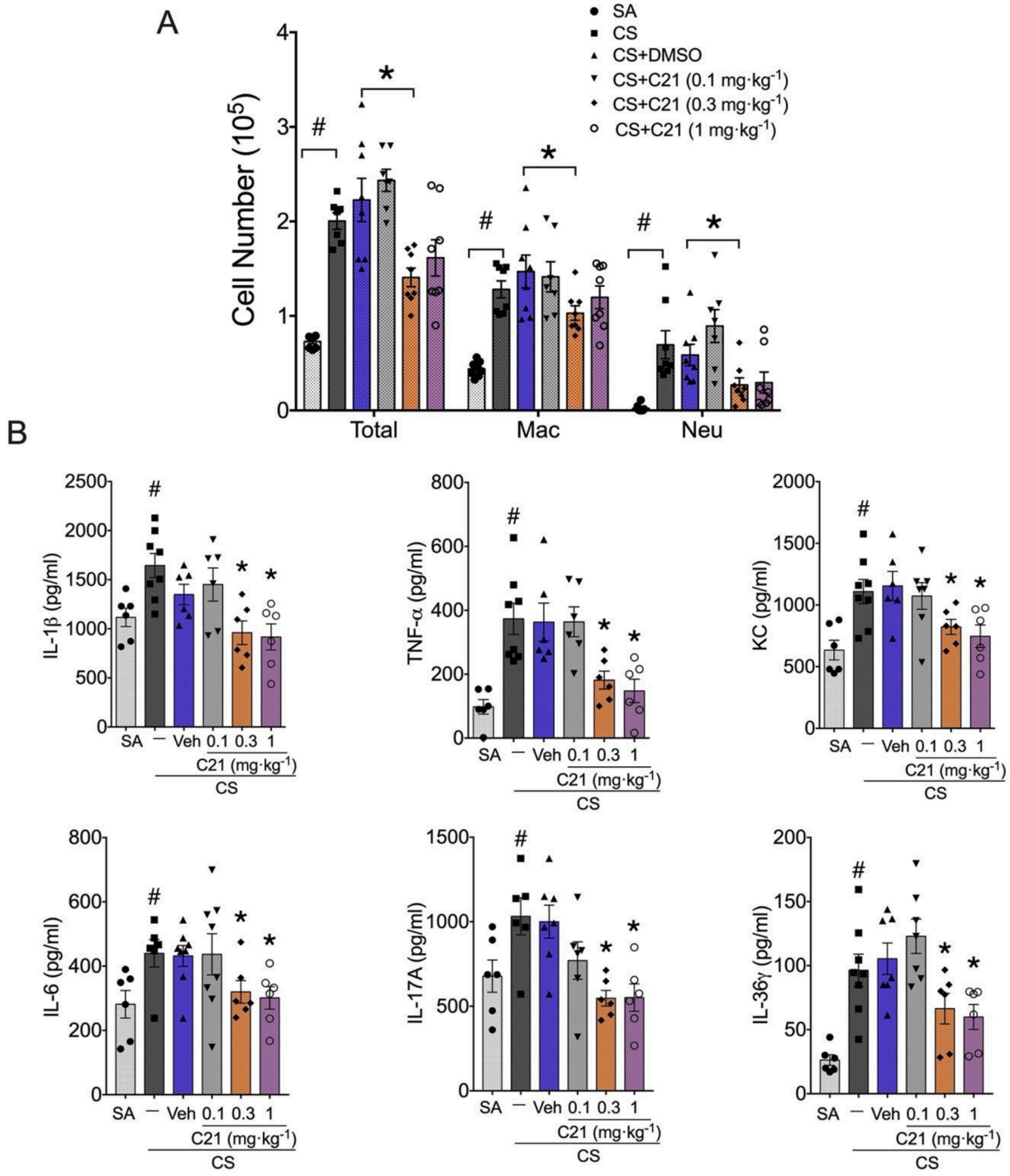

Fig. 2. Anti-inflammatory effects of AT2R agonist C21 in a CS-induced acute lung injury mouse model. (A) Inhibitory effects of C21 on total, macrophage and neutrophil counts in BAL fluid from CS-challenged mice (n = 6-8). (B) Inhibitory effects of C21 on pro-inflammatory cytokine levels in BAL fluid from CS-challenged mice (n = 6-8). Values are expressed as mean ± SEM. #: $p < 0.05$ compared with sham air control, *: $p < 0.05$ compared with vehicle DMSO control.

and noticeably enhanced Ang 1–7 level (Fig. 1C). Acute CS exposure or C21 treatment had no obvious effect on ACE, ACE2 or AT1R levels in the lungs. However, acute CS challenge slightly reduced AT2R level and evidently lowered Mas receptor level, but C21 (0.3 and 1 mg· kg^{-1}) restored AT2R and Mas receptor levels (Fig. 1D).

3.2. AT2R activation attenuates acute CS-induced airway inflammation

C21 markedly inhibited the acute CS-induced increases in BAL fluid levels of total cell, macrophage and neutrophil counts, to a statistically significant level at a dose of 0.3 mg· kg^{-1} (Fig. 2A). Besides, C21 dose-dependently blocked acute CS-induced surge in BAL fluid levels of pro-inflammatory cytokines including IL-1β, TNF-α, KC, IL-6, IL-17A and IL-36γ (Fig. 2B). C21 treatments did not alter complete blood count, or serum levels of AST/ALT and creatinine, in all mice (data not shown).

3.3. AT2R activation attenuates acute CS-induced oxidative damage and airway remodeling

C21 dose-dependently abated acute CS-induced elevation of

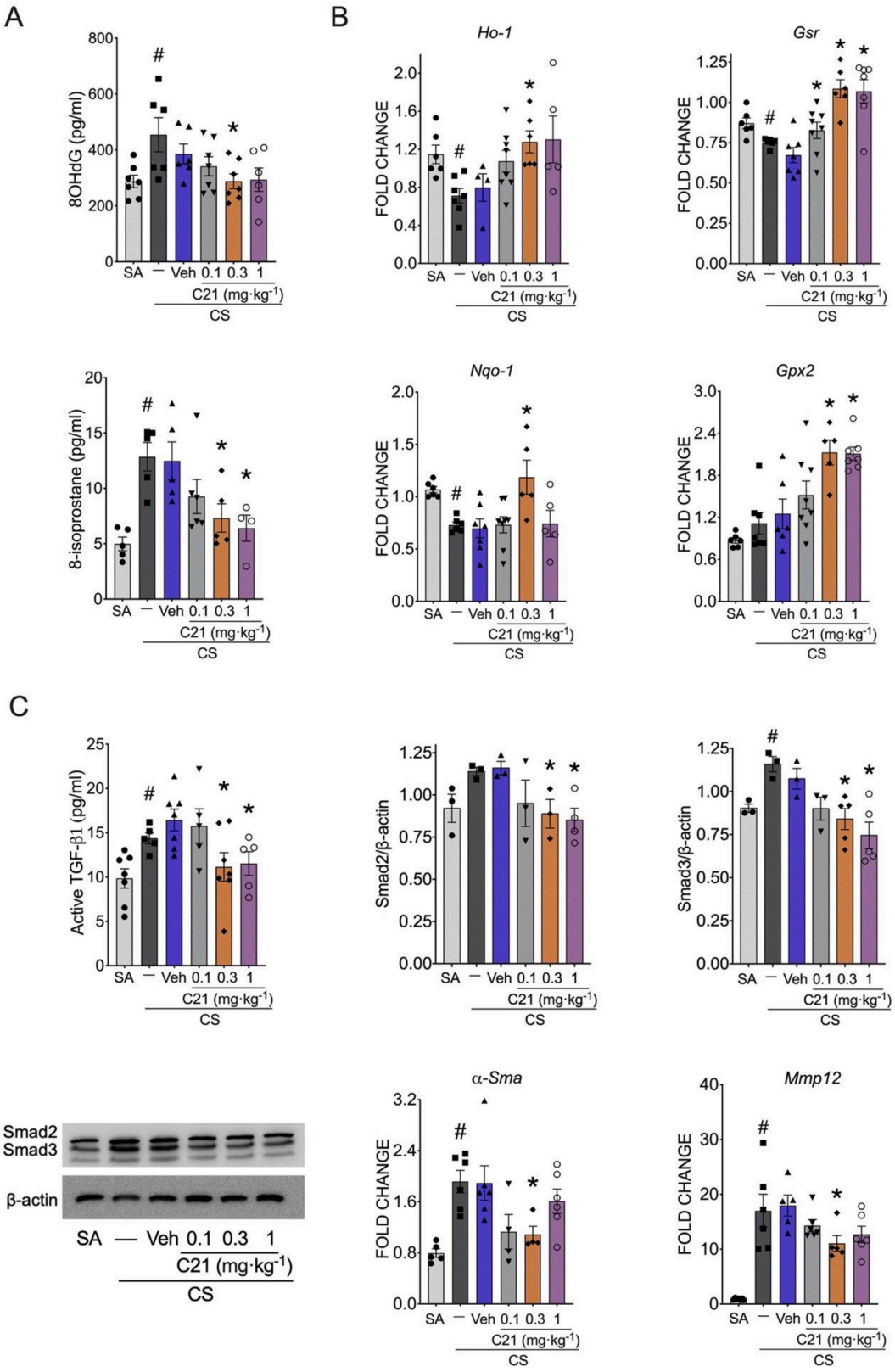

Fig. 3. Anti-oxidative and anti-remodeling effects of AT2R agonist C21 in a CS-induced acute lung injury mouse model. (A) Inhibitory effects of C21 on oxidative damage markers in BAL fluid from CS-exposed mice (n = 4-7). (B) Effects of C21 on *Ho-1, Gsr, Nqo-1* and *Gpx2* expression in lung tissues from CS-exposed mice (n = 4-8). (C) Inhibitory effects of C21 on active TGF-β1 level (n = 5-7), smad2 and smad3 levels (n = 3-5), and gene expression of *α-Sma* (n = 4-6) and *Mmp12* (n = 5-7), in lung tissues from CS-challenged mice. Values are expressed as mean ± SEM. #: $p < 0.05$ compared with sham air control, *: $p < 0.05$ compared with vehicle DMSO control.

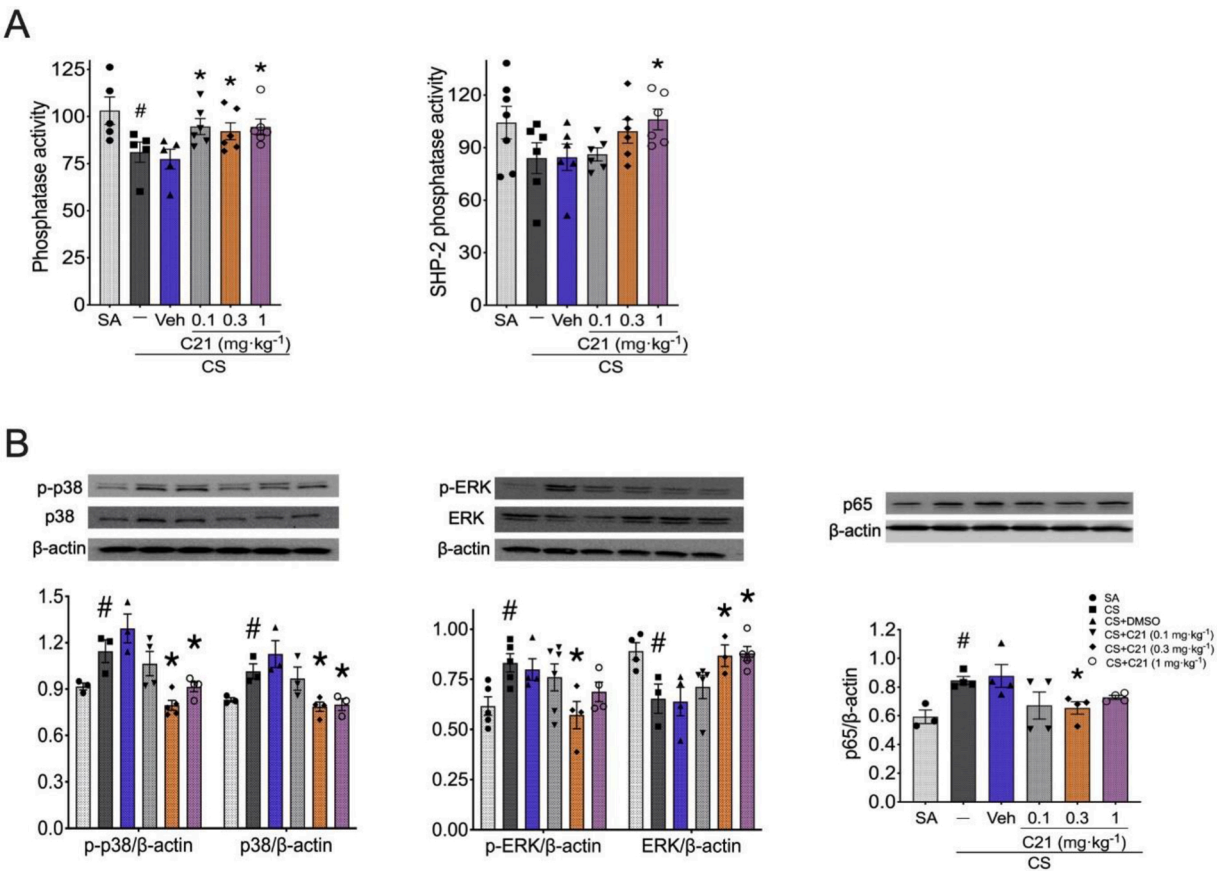

Fig. 4. Mechanisms of action of AT2R agonist C21 in a CS-induced acute lung injury mouse model. (A) Restorative effects of C21 on CS-induced reduction of phosphatase activities in lung tissues from CS-challenged mice (n = 5-7). (B) Effects of C21 on phospho-p38 MAPK, p38 MAPK, phospho-ERK, ERK and p65 subunit of NF-κB levels in lung tissues from CS-challenged mice (n = 3-5). Values are expressed as mean ± SEM. #: $p < 0.05$ compared with sham air control, *: $p < 0.05$ compared with vehicle DMSO control.

oxidative damage markers 8−OH-2′-deoxyguanosine (8−OHdG) and 8-isoprostane in the BAL fluid (Fig. 3A). The inhibitory effects of C21 are associated with the restoration of antioxidant gene expression of heme oxygenase 1 (*Ho-1*), NADPH:quinone oxidoreductase 1 (*Nqo-1*) and glutathione-disulfide reductase (*Gsr*), and up-regulation of glutathione peroxidase 2 (*Gpx2*), in CS-exposed lungs (Fig. 3B). Acute CS markedly increased lung tissue levels of active TGF-β1 and of transcription factors smad2 and smad3 (Fig. 3C), which mediate TGF-β receptor signaling response [28]. C21 reduced the levels of TGF-β1 and smad2/3 in a dose-dependent manner (Fig. 3C). Correspondingly, C21 reverted acute CS-induced increase in α-smooth muscle actin (*α-Sma*) and matrix metalloproteinase 12 (*Mmp12*) in lung tissues (Fig. 3C).

3.4. AT2R activation modulates acute CS-induced signaling responses

AT2R activation has been shown to activate phosphatase activities [10,11]. CS exposure noticeably diminished total phosphatase and slightly diminished SH2-domain-containing phosphatase-2 (SHP-2) activities, and C21 regenerated phosphatase activity in the lungs (Fig. 4A). CS challenge markedly upregulated total p38 MAPK, phospho-p38 MAPK, phospho-ERK and p65 subunit of NF-κB levels in the lungs, while down-regulated total ERK level. C21 was able to repress the protein levels of total p38 MAPK, phospho-p38 MAPK, phospho-ERK and p65 subunit of NF-κB to the baseline, and conversely restored total ERK level to basal level (Fig. 4B).

3.5. AT2R activation modulates RAS in chronic CS-induced COPD

As the C21 dose of 0.3 mg· kg^{-1} has demonstrated consistent protective effects in the acute CS-induced lung injury model, we have selected this effective dose to study potential benefits of C21 in the chronic CS-induced COPD model (Fig. 5A). Chronic CS challenge markedly up-regulated Ang I, Ang II and Ang-(1–7) levels in lung tissues. C21 differentially modulated Ang I and Ang II down to basal levels, but up Ang-(1–7) to a higher level (Fig. 5B). Chronic CS exposure significantly increased ACE and ACE2 levels in the lungs, but C21 repressed their protein levels down to baseline controls (Fig. 5C). Chronic CS down-regulated AT1R and Mas receptors in the lungs, but elevated AT2R level. C21 treatment was able to reverse the alterations induced by CS on these receptors to their basal levels (Fig. 5C).

3.6. AT2R activation attenuates chronic CS-induced airway inflammation

C21 significantly inhibited the chronic CS-induced increases in BAL fluid total cell, macrophage and neutrophil counts (Fig. 6A). In addition, C21 blocked chronic CS-induced rise in BAL fluid pro-inflammatory cytokines including TNF-α, KC, IL-6 and IL-17A (Fig. 6B). Furthermore, C21 reduced chronic CS-induced inflammatory cell infiltration and epithelial thickening (Fig. 6C). Chronic CS exposure markedly increased *Muc5b* gene expressions in lung tissues, with minor effect on *Muc5ac*, and C21 significantly reduced pulmonary gene expression of *Muc5b* (Fig. 6D).

3.7. AT2R activation attenuates chronic CS-induced airway remodeling

Chronic CS significantly increased lung tissue levels of active TGF-β1 and of transcription factors smad2 and smad3 (Fig. 7A). C21 repressed the levels of TGF-β1 and smad2/3 to the basal levels (Fig. 7A).

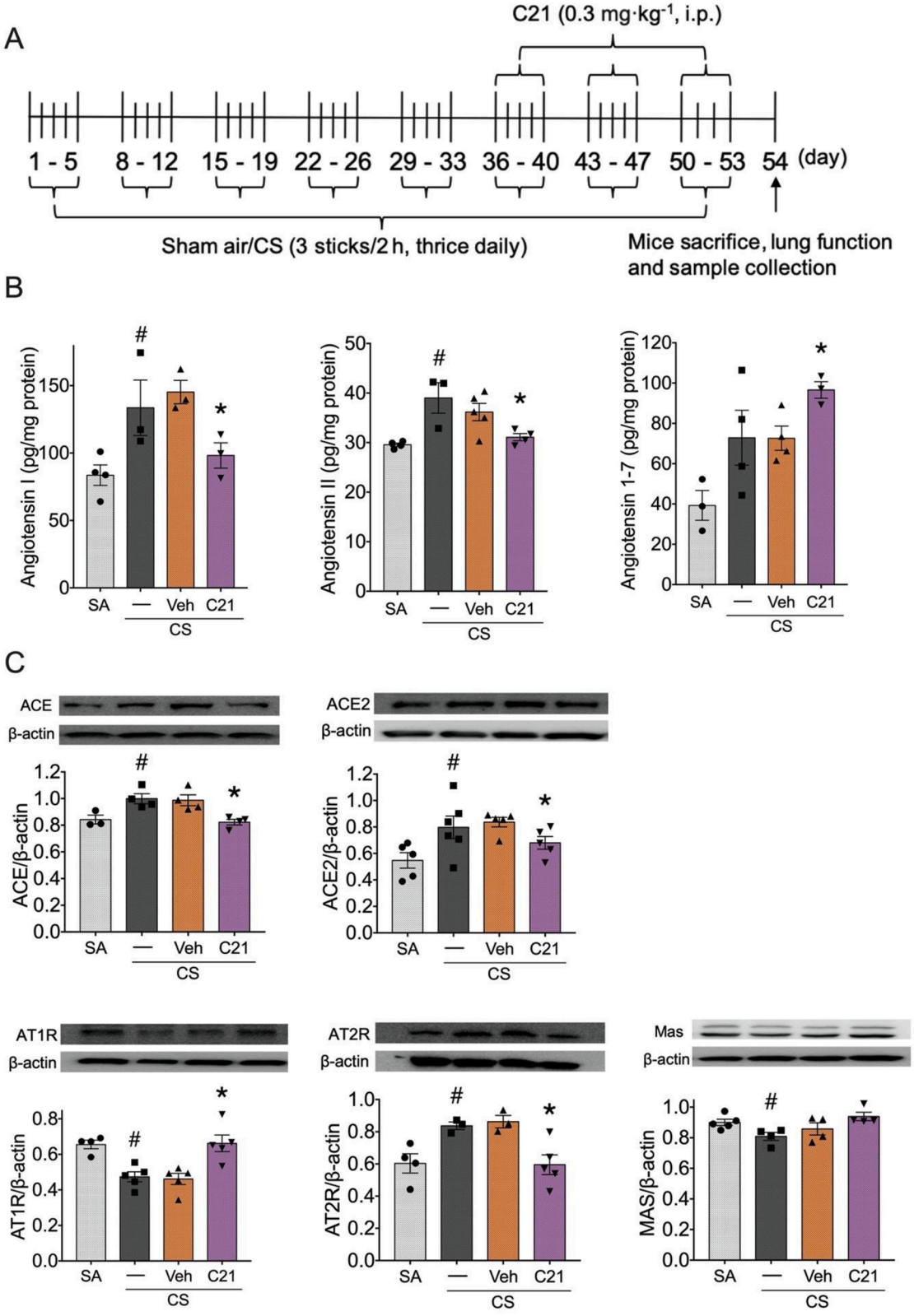

Fig. 5. Modulatory effects of AT2R agonist C21 on RAS in a chronic CS-induced COPD mouse model. (A) Experimental protocol for the 8-week CS-induced chronic COPD mouse model. C21 was given once daily 1 h before CS exposure. (B) Effects of C21 on the levels of Ang I, Ang II and Ang-(1-7) in lung tissues from CS-challenged mice (n = 3-5). (C) Effects of C21 on the expression of ACE, ACE2, AT1R, AT2R and Mas receptor in lung tissues from CS-challenged mice (n = 3-5). Values are expressed as mean ± SEM. #: $p < 0.05$ compared with sham air control, *: $p < 0.05$ compared with vehicle DMSO control.

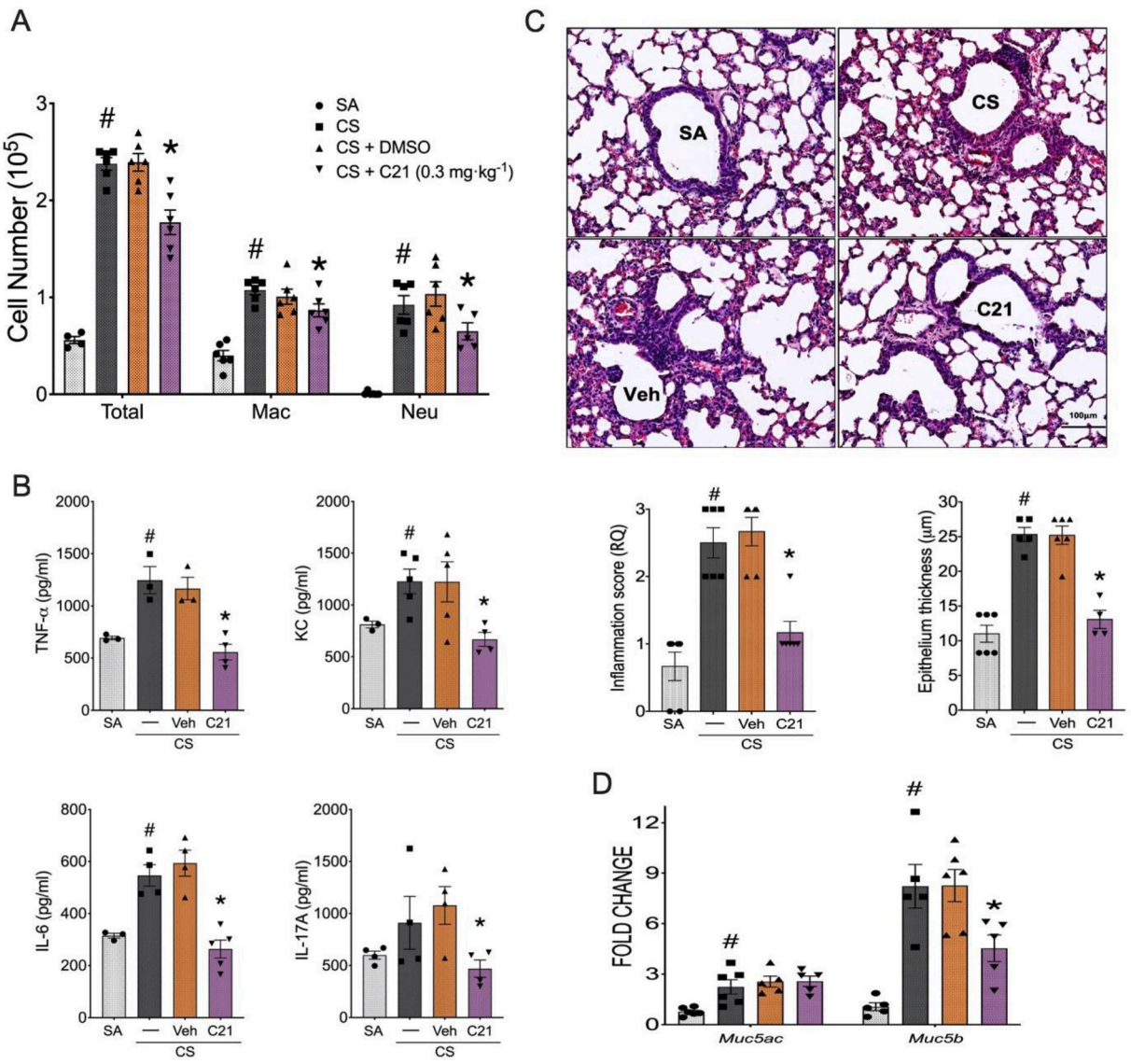

Fig. 6. Anti-inflammatory effects of AT2R agonist C21 in a chronic CS-induced COPD mouse model. (A) The inhibitory effects of C21 on total, macrophage and neutrophil cell counts in BAL fluid from CS-challenged mice (n = 4-6). (B) Inhibitory effects of C21 on pro-inflammatory cytokine levels in BAL fluid from CS-challenged mice (n = 3-5). (C) Inhibitory effects of C21 on bronchial epithelium thickness and inflammation in lung tissues from CS-challenged mice (n = 4-6). (D) Effects of C21 on *Muc5ac* and *Muc5b* gene expressions in lung tissues from CS-challenged mice (n = 5-6). Values are expressed as mean ± SEM. #: $p < 0.05$ compared with sham air control, *: $p < 0.05$ compared with vehicle DMSO control.

Correspondingly, C21 reverted chronic CS-induced increase in *α-Sma* in lung tissues (Fig. 7A). Besides, C21 significantly abated chronic CS-induced elevation of NE activity in BAL fluid, and hydroxyproline level, *Mmp9* and *Mmp12* gene expression in lung tissues (Fig. 7B). Furthermore, C21 was able to augment CS-induced elevation of tissue inhibitor of metalloproteinase-1 (*Timp-1*) expression in lung tissues (Fig. 7B).

3.8. AT2R activation mitigates chronic CS-induced emphysema and lung function impairment

Chronic CS exposure induced obvious enlargement of alveoli measured as increases in alveolar diameter, and C21 was able to significantly reduce alveolar enlargement (Fig. 8A). Chronic CS exposure decreased forced expiratory volume in 100 ms over forced vital capacity ratio (FEV_{100}/FVC, equivalent to FEV_1/FVC ratio in humans), inspiratory capacity (IC) and dynamic compliance (Cdyn), but increased total lung capacity (TLC), functional residual capacity (FRC) and static compliance (Cchord) (Fig. 8B). C21 significantly mitigated TLC, FRC and Cchord, and restored FEV_{100}/FVC, IC and Cdyn in chronic CS-challenged mice.

4. Discussion

In both acute and chronic CS models, Ang I and Ang II were markedly elevated in the lungs. While Ang II can bind to AT1R and AT2R, it is the AT1R activation that causes pro-inflammatory, pro-oxidative and pro-fibrotic effects in COPD [11,12]. We observed increases in macrophage and neutrophil counts, oxidative damage markers and pro-inflammatory cytokine levels in the BAL fluid, and inflammatory cell infiltration and epithelial thickness in the lung sections obtained from CS-exposed lungs. AT1R acts through coupling to Gαq/11, Gα12/13 and Gαi, and through receptor transactivation to stimulate multiple signaling processes including p38 MAPK, ERK, NF-κB and NADPH oxidase pathways [10,11]. In the acute CS model, we were able to capture heightened levels of phospho-p38 MAPK, phospho-ERK and

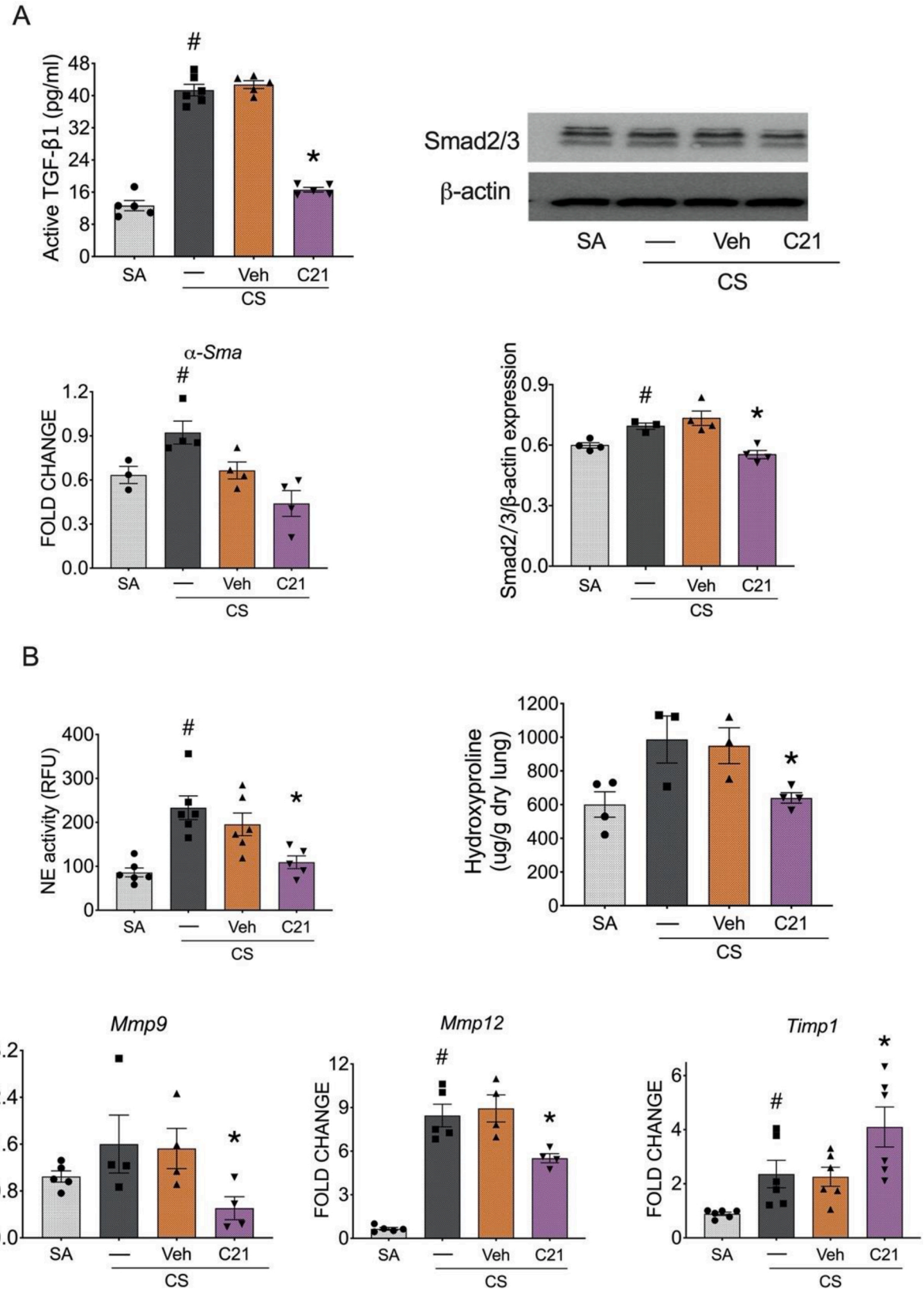

Fig. 7. Anti-remodeling effects of AT2R agonist C21 in a chronic CS-induced COPD mouse model. (A) Inhibitory effects of C21 on active TGF-β1 level (n = 5-6), smad2/3 protein levels, and *α-Sma* gene expression in lung tissues from CS-challenged mice (n = 3-5). (B) Inhibitory effects of C21 on NE activity in BAL fluid (n = 5-6), hydroxyproline level (n = 3-4), *Mmp9* and *Mmp12* gene expression (n = 4-5), and *Timp1* gene expression (n = 6), in lung tissues from CS-challenged mice. Values are expressed as mean ± SEM. #: $p < 0.05$ compared with sham air control, *: $p < 0.05$ compared with vehicle DMSO control.

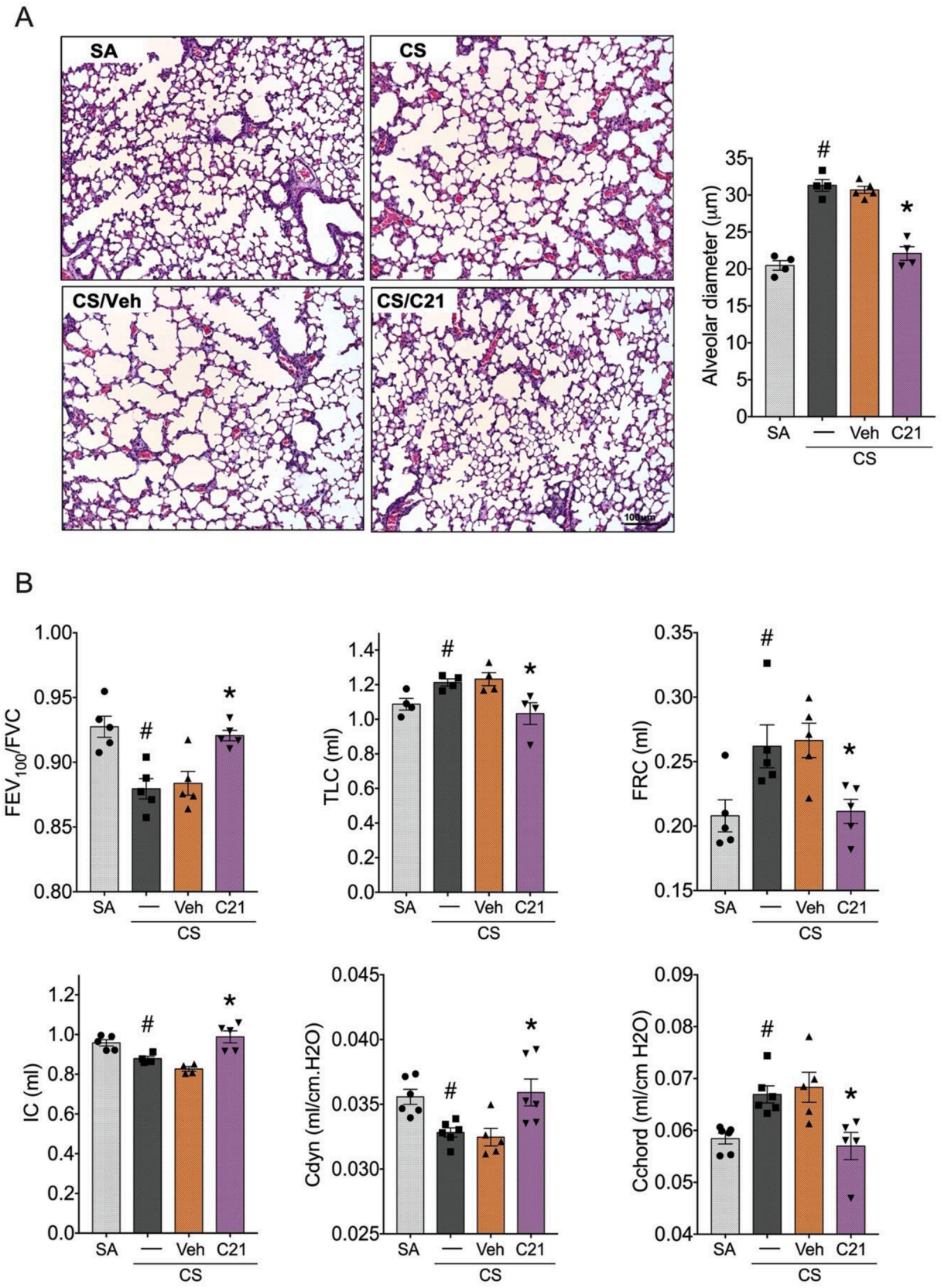

Fig. 8. Protective effects of AT2R agonist C21 on emphysematic damage and lung function impairment in a chronic CS-induced COPD mouse model. (A) Inhibitory effects of C21 on alveolar enlargement in lung tissues from CS-challenged mice (n = 4-5). (B) Effects of C21 on improving lung functions in CS-challenged mice (n = 4-6). Values are expressed as mean ± SEM. #: $p < 0.05$ compared with sham air control, *: $p < 0.05$ compared with vehicle DMSO control.

NF-κB p65 subunit in the lung tissues.

Acute CS challenge did not alter the levels of ACE, ACE2, AT1R and AT2R in the lung tissues; however, chronic CS exposure significantly upregulated ACE, ACE2 and AT2R levels, while downregulated AT1R level in the lungs, indicative of a compensatory response to control airway inflammation. It has been shown that CS-exposed lungs expressed higher levels of ACE2 [29,30], implying more conversion of pro-inflammatory Ang II into anti-inflammatory Ang-(1–7) to counteract CS damage to the lungs. Lately, ACE2 has taken the center stage as the pivotal receptor for coronavirus infection (e.g. SARS-CoV-2) leading to severe acute pulmonary syndrome. COPD patients have higher levels of ACE2, implicating that they are more susceptible to SARS-CoV-2 infection [29–31]. Unexpectedly, C21 was able to lower the ACE2 back to baseline level in chronic CS-exposed lungs. Increased AT2R expression has been reported in inflammation models including idiopathic lung fibrosis [24], rheumatoid arthritis [32] and glomerulonephritis [33]. It has been shown that activation of AT1R upregulated AT2R expression in rat aorta [34]. AT2R is an atypical GPCR that it acts through coupling to Gαi/Gαo as well as Gαs, and through activating G protein-independent pathways like serine/threonine phosphatase 2A, SHP-1 and SHP-2, resulting in anti-inflammatory, anti-proliferative and anti-fibrotic effects [11,35,36]. In this study, AT2R activation by C21 markedly suppressed CS-induced increases in BAL fluid levels of macrophage and neutrophil counts, pro-inflammatory cytokines, and oxidative damage markers 8−OHdG and 8-isoprostane, and in inflammatory cell infiltration, epithelial thickening and *muc5b* expression. Besides, C21 promoted endogenous antioxidant gene expression including *Ho-1*, *Nqo1*, *Gsr* and *Gpx2* to counteract CS-induced oxidative stress. In addition, CS exposure down-regulated phosphatase activities in lung tissues, but C21 was able to restore total phosphatase and SHP-2 activities to normal levels. As a result, we observed that C21 treatment reduced phospho-p38 MAPK and phospho-ERK levels in the CS-exposed lungs.

Both acute CS and chronic CS models markedly elevated TGF-β1 levels and upregulated the lung tissue levels of transcription factors Smad2 and Smad3 which mediate TGF-β1-induced signaling process [28,37]. TGF-β1 release from various cell types such as macrophages, neutrophils and epithelial cells has been shown to be AT1R-dependent [10,11,37]. TGF-β1 is a major pro-fibrotic factor to drive airway remodeling by transdifferentiation of fibroblasts to myofibroblasts and production of extracellular cellular matrices such as collagen [37]. C21 treatment was able to block the CS-induced elevation of TGF-β1 and Smad2/Smad3, and TGF-β1-sensitive *α-Sma* gene expression as well. In the chronic CS model, *Mmp9*, *Mmp12* expression and NE activity were markedly upregulated. They are released from the macrophages and neutrophils, and act by degrading collagen and elastin leading to tissue destruction in the airways [38,39]. C21 noticeably reduced *Mmp9* and *Mmp12* expression, NE activity and the level of hydroxyproline, the major breakdown product of collagen [40]. Besides, C21 augmented the gene expression of *Timp-1*, a critical proteinase inhibitor of MMP9 and MMP12 [41]. In addition, it has been shown that inhibition of p38 MAPK or ERK signaling pathway could block the release of MMP9 from alveolar macrophages [41]. Another possible mechanism of action for C21 is to induce formation of AT2R and AT1R heterodimer resulting in AT1R blockade. Although AT2R *per se* does not undergo receptor desensitization upon Ang II activation, it promotes AT2R-AT1R heterodimer internalization to inhibit AT1R signaling [42,43].

In both acute and chronic mouse models, C21 markedly restored Mas receptors to normal level and augmented the level Ang-(1–7), the endogenous ligand for the Mas receptor [44]. AT2R and Mas receptor are considered the “protective arm” of the RAS, counterbalancing the pro-inflammatory effects of AT1R activation as physiological antagonists [43,45]. Mas receptor is coupled to Gαq, Gαi/s and Gα12 and is constitutively active in producing cAMP [44]. Recent study showed that Ang-(1–7) is a poor G protein activator but it may act via Mas receptors in a yet unknown effector pathway to mediate anti-inflammatory and anti-fibrotic actions [44]. Ang-(1–7) treatment has been shown to attenuate CS-induced lung inflammation, fibrosis and oxidative damage in COPD moues models [19,20]. In addition, Mas receptors can act by forming heterodimers with AT1R to disrupt AT1R signaling responses [45,46]. AT2R and Mas receptor function in a strikingly similar mechanisms, and recent studies have revealed their co-localization and heterodimerization, and functional interdependence in mediating anti-inflammatory actions [36,43,45].

Our findings reveal for the first time the protective effects of AT2R agonist C21 against CS-induced COPD. AT2R is an attractive target for agonist-based therapeutic strategy because AT2R per se is resistant to receptor uncoupling and internalization due to fewer serine/threonine residues located in the carboxyl-terminal [46]. This property offers multiple treatment benefits including minimum dosage requirement, minimum drug tolerance development, and minimum dose-related side effects. In addition, as AT2R level is low in normal situation but highly upregulated in pathophysiological conditions such as inflammation, therapeutic efficacy of AT2R agonist is expected to be the highest during inflammatory phase, and upon resolution phase, AT2R level will decline, and as such the dose requirement and potential AT2R-related side effects will be minimized as well. The present study provides strong scientific evidence for further development of AT2R agonist, such as C21, for the treatment of COPD.

Transparency document

The Transparency document associated with this article can be found in the online version.

Declaration of Competing Interest

None.

Acknowledgments

This work was supported by a grant from the Singapore National Research Foundation (NRF/CREATE/R-184-000-269-592 to W.S.F.W) and a PhD research scholarship (201706220119) by the China Scholarship Council to D.M.

Appendix A. Supplementary data

Supplementary material related to this article can be found, in the online version, at doi:https://doi.org/10.1016/j.phrs.2020.105223.

References

[1] A. Augusti, J.C. Hogg, Update on the pathogenesis of chronic obstructive pulmonary disease, N. Engl. J. Med. 381 (2019) 1248–1256.
[2] B.R. Celli, J.A. Wedzicha, Update on clinical aspects of chronic obstructive pulmonary disease, N. Engl. J. Med. 381 (2019) 1257–1266.
[3] S. Boukhenouna, M.A. Wilson, K. Bahmed, et al., Reactive oxygen species in chronic obstructive pulmonary disease, Oxid. Med. Cell. Longev. (2018) 5730395.
[4] L. Vanhamme, K.Z. Boudjeltia, P. Van-Antwerpen, et al., The other myeloperoxidase: emerging functions, Arch. Biochem. Biophys. 649 (2018) 1–14.
[5] P.J. Barnes, Oxidative stress-based therapeutics in COPD, Redox Biol. 33 (2020) 101544.
[6] L.E.S. de Groot, T.A. van der Veen, F.O. Martinez, et al., Oxidative stress and macrophages: driving forces behind exacerbation of asthma and chronic obstructive pulmonary disease? Am. J. Physiol. Lung Cell Mol. Physiol. 316 (2019) L369–L384.
[7] A.E. Jasper, W.J. Mclver, E. Sapey, et al., Understanding the role of neutrophils in chronic inflammatory airway disease, F1000Research 8 (2019) 557.
[8] D. Mei, W.S.D. Tan, W.S.F. Wong, Phamacological strategies to regain steroid sensitivity in severe asthma and COPD, Curr. Opin. Pharmacol. 46 (2019) 73–81.
[9] M. Bader, Tissue renin-angiotensin-aldosterone systems: targets for pharmacological therapy, Annu. Rev. Pharmacol. Toxicol. 50 (2010) 439–465.
[10] S.J. Forrester, G.W. Booz, C.D. Sigmund, et al., Angiotensin II signal transduction: an update on mechanisms of physiology and pathophysiology, Physiol. Rev. 98 (2018) 1627–1738.
[11] D.G. Passos-Silva, E. Brandan, R.A. Santos, Angiotensins as therapeutic targets beyond heart disease, Trends Pharmacol. Sci. 36 (2015) 310–320.

[12] W.S.D. Tan, W. Liao, S. Zhou, et al., Targeting the renin-angiotensin system as novel therapeutic strategy for pulmonary disease, Curr. Opin. Pharmacol. 40 (2018) 9–17.
[13] T. Raupach, L. Luthje, H. Kogler, et al., Local and systemic effects of angiotensin receptor blockade in an emphysema mouse model, Pulm. Pharmacol. Ther. 24 (2011) 215–220.
[14] M. Podowski, C. Calvi, S. Metzger, et al., Angiotensin receptor blockade attenuates cigarette smoke–induced lung injury and rescues lung architecture in mice, J. Clin. Invest. 122 (2012) 229–240.
[15] M.A. Parikh, C.P. Aaron, E.A. Hoffman, et al., Angiotensin-converting inhibitors and angiotensin II receptor blockers and longitudinal change in percent emphysema on computed tomogaphy, Ann. Am. Thoracic Soc. 14 (2017) 649–658.
[16] J. Kim, J.K. Lee, E.Y. Heo, et al., The association of renin-angiotensin system blockades and pneumonia requiring admission in patients with COPD, Int. J. Chron. Obstruct. Pulm. Dis. 11 (2016) 2159–2166.
[17] P. Paulin, J.M. Furcada, C.M. Ungaro, et al., Effect of angiotensin 2 receptor blockers on chronic obstructive lung disease mortality: a retrospective cohort study, Pulm. Pharmacol. Ther. 44 (2017) 78–82.
[18] A.C. Bastos, G.S. Magalhaes, J.F. Gregorio, et al., Oral formulation of angiotensin-(1-7) therapy attenuates pulmonary and systemic damage in mice with emphysema induced by elastase, Immunobiology 225 (2020) 151893.
[19] Y. Zhang, Y. Li, C. Shi, et al., Angiotensin-(1-7)-mediated Mas1 receptor/NF-κB-p65 signaling is involved in a cigarette smoke-induced chronic obstructive pulmonary disease mouse model, Environ. Toxicol. 33 (2018) 5–15.
[20] M. Pan, Z. Zheng, Y. Chen, et al., Angiotensin-(1-7) attenuated cigarette smoking-related pulmonary fibrosis via improving the impaired autophagy caused by nicotinamide adenine dinucleotide phosphate reduced oxidase 4-dependent reactive oxygen species, Am. J. Physiol. Lung Cell Mol. Physiol. 59 (2018) 306–319.
[21] M. Hallberg, C. Sumners, U.M. Steckelings, et al., Small-molecule AT2 receptor agonists, Med. Res. Rev. 38 (2018) 602–624.
[22] S. Bosnyak, E.S. Jones, A. Christopoulos, et al., Relative affinity of angiotensin peptides and novel ligands at AT1 and AT2 receptors, Clin. Sci. 121 (2011) 297–303.
[23] S. Vasile, A. Hallberg, J. Sallander, et al., Evolution of angiotensin peptides and peptidomimetics as angiotensin II receptor type 2 (AT2) receptor agonists, Biomolecules 10 (2020) 649.
[24] A. Rathinasabapathy, A. Horowitz, K. Horton, et al., The selective angiotensin II type 2 receptor agonist, compound 21, attenuates the progression of lung fibrosis and pulmonary hypertension in an experimental model of bleomycin-induced lung injury, Front. Physiol. 9 (2018) 180.
[25] U. Steckelings, L. Lindblad, A. Leisvuori, et al., Successful completion of a phase I, randomized, double-blind, placebo controlled, single ascending dose trial for the first in class angtiotensin AT2-receptor agonist compound 21, J. Hypertension 35 (2017) e105–e106.
[26] H.Y. Peh, W.S.D. Tan, T.K. Chan, et al., Vitamin E isoform γ-tocotrienol protects against emphysema in cigarette smoke-induced COPD, Free Radic. Biol. Med. 110 (2017) 332–344.
[27] J. Dong, W. Liao, H.Y. Peh, et al., Ribosomal protein S3 gene silencing protects against cigarette smoke-induced acute lung injury, Mol. Ther. Nucleic Acids 12 (2018) 370–380.
[28] H. Khalil, O. Kanisicak, V. Prasad, et al., Fibroblast-specific TGF-β–Smad2/3 signaling underlies cardiac fibrosis, J. Clin. Invest. 127 (2017) 3770–3783.
[29] G. Cai, Y. Bosse, F. Xiao, et al., Tobacco smoking increaseses the lung gene expression of ACE2, the receptor of SARS-CoV-2, Am. J. Respir. Crit. Care Med. 201 (2020) 1557–1559.
[30] J.M. Leung, C.X. Yang, A. Tam, et al., ACE-2 expression in the small airway epithelia of smokers and COPD patients: implications for COVID-19, Eur. Respir. J. 55 (2020) 2000688.
[31] J.C. Smith, E.L. Sausville, V. Girish, et al., Cigarette smoke exposure and inflammatory signaling increase the expression of the SARS-CoV-2 receptor ACEs in the respiratory tract, Dev. Cell 53 (2020) 514–529.
[32] R. Terenzi, M. Manetti, I. Rosa, et al., Angiotensin II type 2 receptor (AT2R) as a novel modulator of inflammation in rheumtoid arthritis synovium, Sci. Rep. 7 (2017) 13293.
[33] H. Okada, T. Inoue, T. Kikut, et al., A possible anti-inflammatory role of angiotensin II type 2 receptor in immune-mediated glomerulonephritis during type 1 receptor blockade, Am. J. Pathol. 169 (2006) 1577–1589.
[34] K. Yayama, M. Horii, H. Hiyoshi, et al., Up-regulation of angiotensin II type 2 receptor in rat thoracic aorta by pressure-overload, J. Pharmacol. Exp. Ther. 308 (2004) 736–743.
[35] Y.H. Lee, O. Mungunsukh, R.L. Tutino, et al., Angiotensin-II-induced apoptosis requires regulation of nucleolin and Bcl-x_L by SHP-2 in primary lung endothelial cells, J. Cell. Sci. 123 (2010) 1634–1643.
[36] D. Villela, J. Leonhardt, N. Patel, et al., Angiotensin type 2 receptor (AT2R) and receptor Mas: a complex liaison, Clin. Sci. 128 (2015) 227–234.
[37] Y. Wang, M. Del Borgo, H.W. Lee, et al., Anti-fibrotic potential of AT2 receptor agonists, Front. Pharmacol. 8 (2017) 564.
[38] A. Churg, S. Zhou, J.L. Wright, Matrix metalloproteinases in COPD, Eur. Respir. J. 39 (2012) 197–209.
[39] K.C. Pandey, S. De, P.K. Mishra, Role of proteases in chronic obstructive pulmonary disease, Front. Pharmacol. 8 (2017) 512.
[40] C. Martin-Mosquero, G. Peces-Barba, M.L. Rubio, et al., Increased collagen deposition correlated with lung destruction in human emphysema, Histo. Histopathol. 21 (2006) 823–828.
[41] C.Y. Lo, H.Y. Huang, J.R. He, et al., Increased matrix metalloproteinase-9 to tissue inhibitor of metalloproteinase-1 ratio in smokers with airway hyperresponsiveness and accelerated lung function decline, Int. J. COPD 13 (2018) 1135–1144.
[42] T. Inuzuka, Y. Fujioka, M. Tsuda, et al., Attenuation of ligand-induced activation of angiotensin II type 1 receptor signaling by the type 2 receptor via protein kinase C, Sci. Rep. 6 (2016) 21613.
[43] J. Leonhardt, D.C. Villela, A. Teichmann, et al., Evidence for heterodimerization and functional interaction of the angiotensin type 2 receptor and the receptor MAS, Hypertension 69 (2017) 1128–1135.
[44] K.C. Tirupula, R. Desnoyer, R.C. Speth, et al., Atypical signaling and functional desensitization response of MAS receptor to peptide ligands, PLoS One 9 (2014) e103520.
[45] S. Patel, T. Hussain, Dimerization of AT 2 and Mas receptors in control of blood pressure, Curr. Hypertens. Rep. 20 (2018) 41.
[46] E. Kostenis, G. Milligan, A. Christopoulos, et al., G-protein-coupled receptor Mas is a physiological antagonist of angiotensin II type 1 receptor, Circulation 111 (2005) 1806–1813.